Contrib Mineral Petrol (2002) 144: 274–285
DOI 10.1007/s00410-002-0400-7

ORIGINAL PAPER

Jorge A. Vazquez · Mary R. Reid

Time scales of magma storage and differentiation of voluminous high-silica rhyolites at Yellowstone caldera, Wyoming

Received: 7 March 2002 / Accepted: 7 July 2002 / Published online: 26 September 2002

Abstract Ion microprobe dating of zircons from post-collapse rhyolites at Yellowstone caldera reveals the time scales of crystallization and storage of silicic magma in a differentiating magma reservoir, the role of recycling of crystals from the caldera-forming magmatism, and the timing and efficacy of crystal-melt separation. Zircons in the voluminous (~900 km^3) Central Plateau Member lavas, which progressively erupted between 70 to 160 ka, yield $^{238}U - ^{230}Th$ disequilibrium ages dominantly spanning the range from those of their respective eruptions to ~200 ka; mean zircon ages range to ca. 60,000 years before eruption. When considered together with the trace element and Sr- and Nd-isotope compositions of their host melts, the age distributions of the CPM zircons show that the rhyolites are cogenetic and differentiated tens of thousands of years prior to eruption from an evolving magma reservoir. Thus, the post-caldera CPM rhyolites were not erupted from a long-standing body of rhyolitic magma left over from the caldera-forming eruption, nor do they represent significant remobilization of the plutonic roots of the caldera. Rather, the CPM magma was generated and differentiated by episodes of effective crystal-melt separation at ~200 and ~125 ka and, sustained by thermal inputs, stored for timescales on par with estimates for other voluminous caldera-related rhyolites.

Introduction

Determining the pre-eruptive history of magma is fundamental to understanding the magmatic evolution that leads to volcanic eruptions. This history is especially important in the case of restless calderas where little is known about the time scales of magma accumulation and storage prior to large eruptions, and where differentiated magmas such as rhyolite might erupt explosively (Newhall and Dzurisin 1988). Rhyolites can be chemically linked by trace element trends and/or isotopic fingerprints, but these characteristics usually provide little and often ambiguous information about the time scales of storage and differentiation prior to eruption, and the efficacy of crystal–liquid separation. In amenable cases, estimates of differentiation and storage time scales for caldera-related rhyolites have been made by mineral dating. Resulting storage time estimates for some voluminous (> 100 km^3) caldera-forming rhyolites are < 100,000 years and, where applicable, less than the repose interval between successive caldera-forming eruptions (e.g., Charlier and Zellmer 2000; Reid and Coath 2000; Bindeman et al. 2001). In contrast, high-silica rhyolites erupted as small volume lavas in a caldera setting may have pre-eruptive storage periods of > 100,000 years (e.g., Davies et al. 1994; Reid et al. 1997; Davies and Halliday 1998; Heumann et al. 2002). These storage times are longer than the repose interval between their eruptions, suggesting that a single magma reservoir may be tapped repeatedly. The fact that magma storage times do not apparently increase with increasing eruptive volume shows that the size of an eruption is not simply a function of the duration of magma accumulation and evolution (cf. Smith 1979; Trial and Spera 1990), and begs the question of whether the type of eruption is related in any way to the physicochemical pathways of differentiation. To better unravel the relationships between the timing and duration of differentiation and the volume of magma produced, we investigated the crystallization history of voluminous rhyolites erupted periodically from a magma chamber in a caldera setting.

Using primarily ion microprobe $^{238}U–^{230}Th$ ages of zircons from lavas of the Central Plateau Member (CPM) of the Plateau Rhyolite at Yellowstone caldera, we place unique constraints on the crystallization history

J.A. Vazquez (✉) · M.R. Reid
Department of Earth and Space Sciences,
University of California, Los Angeles,
Los Angeles, CA 90095-1567, USA
E-mail: jvazquez@ess.ucla.edu

Editorial responsibility: T.L. Grove

of a suite of rhyolites, which, based on previous work (Christiansen 1984a, 2001; Hildreth et al. 1984), could be related by progressive differentiation. Although the volume of erupted magma is comparable with that of large ignimbrites, the CPM rhyolites erupted over an interval of ~90,000 years, primarily as a series of large-volume lava flows. Thus, rather than a single and instantaneous glimpse into a climactic magma chamber, the CPM rhyolites provide "snapshots" in space and time into a voluminous and evolving magma reservoir. The resulting zircon age distributions and isotopic characteristics support the inference that the CPM rhyolites are cogenetic and constrain the time scales of differentiation and concomitant crystallization to several tens of thousands of years. Moreover, they show that there may be little crystal memory between caldera-forming and post-collapse magmas as well as, in some instances, between otherwise cogenetic rhyolite from one eruption to the next. The CPM magma was stored for time scales comparable with or less than estimates for more- and less-voluminous rhyolites erupted from other long-lived caldera systems, and was apparently accompanied by progressive differentiation, punctuated by episodic and effective crystal–liquid separation.

Central Plateau Member rhyolites and Yellowstone caldera

The Central Plateau Member rhyolites are the youngest magmas erupted from the Yellowstone Plateau volcanic field of western Wyoming–eastern Idaho. Since 2.1 Ma, three volcanic cycles have erupted more than 6,000 km^3 of rhyolitic magma and resulted in the collapse of three large calderas in the Yellowstone Plateau volcanic field (Christiansen 1982, 1984b, 2001). Based on secular geochemical and isotopic relations (Hildreth et al. 1984, 1991) and eruptive histories (Christiansen 2001), each cycle has been interpreted to result from the accumulation, storage, and differentiation of discrete silicic magma reservoirs. The youngest cycle culminated with collapse of Yellowstone caldera at 639 ± 2 ka (Lanphere et al. 2002) and emplacement of the ~1,000 km^3 Lava Creek Tuff (Christiansen 1982). The floor of Yellowstone caldera has been subsequently filled by rhyolite lavas and lesser tuffs primarily composing the Upper Basin and Central Plateau Members of the Plateau Rhyolite (Fig. 1; Christiansen and Blank 1972). Upper Basin Member (UBM) rhyolites (72–76 wt% SiO_2) were mostly erupted ~150,000 years after the Lava Creek Tuff (Christiansen 1984a; Gansecki et al. 1996). The UBM represents either contamination of residual Lava Creek Tuff magma (Hildreth et al. 1984, 1991), or localized melting of wallrock by a resident subcaldera magma reservoir (Bindeman and Valley 2000). After a hiatus of about 300,000 years, the Scaup Lake flow, considered to be the youngest and most-evolved UBM lava, erupted at ~200 ka (Christiansen 1984a; Gansecki et al. 1996). Eruption of the CPM occurred between

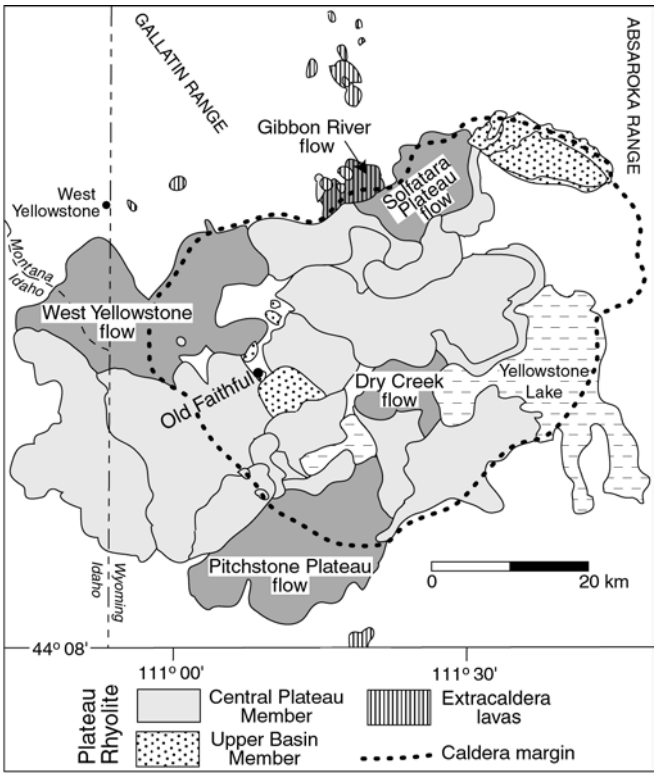

Fig. 1 Yellowstone caldera and associated Plateau Rhyolite lavas and tuffs. Sampled lavas are *shaded*. The Mallard Lake Member (1 lava) is included with the CPM rhyolites. Modified from Hildreth et al. (1984) and Christiansen (2001)

~160 and 70 ka and produced more than 900 km^3 of voluminous lava flows and minor tuff units (Christiansen 1984a, 2001; Obradovich 1992). CPM lavas are high-silica rhyolites (≥76 wt% SiO_2) and are geochemically and mineralogically the most evolved of the post-collapse rhyolites (Christiansen 1984a). A bimodal suite of post-collapse rhyolite and basalt lavas, isotopically distinct from nearby intracaldera lavas, vented outside of the caldera margins (Doe et al. 1982; Hildreth et al. 1984, 1991). An absence of basalt within the caldera floor suggests capture of rising mafic magma by a persistent subcaldera system of partially molten rhyolite (Christiansen 1984a, 1984b, 2001).

Samples and methods

Four CPM lavas (Dry Creek, West Yellowstone, Solfatara Plateau, and Pitchstone Plateau flows) that cover a range of eruption ages (K–Ar sanidine ages of 160 ± 2, 120 ± 3, 110 ± 3, and 70 ± 2, respectively; Obradovich 1992) and bracket the eruptive stratigraphy were chosen for ion microprobe analysis. These lavas erupted from different portions of the caldera (Fig. 1), and in the cases of Pitchstone Plateau and West Yellowstone, represent some of Yellowstone's largest rhyolite lava flows. One extracaldera lava (Gibbon River flow; K–Ar sanidine age of 90 ± 2 ka; Obradovich 1992) was also analyzed for

comparison. The mineralogy of the samples includes 10–30% sanidine, quartz, clinopyroxene, Fe–Ti oxides, fayalite, and rare plagioclase, as well as trace amounts of zircon, chevkinite, and allanite. Zircons in the lavas range from 60–300 μm in length (average ~100 μm) and are dominantly euhedral microphenocrysts in groundmass glass, as well as inclusions in mafic silicate and oxide phenocrysts (Fig. 2); the largest zircons occur in the West Yellowstone and Gibbon River flows. With one exception, the analyzed zircons are euhedral, and clear to slightly cloudy; a rare, cloudy grain from the West Yellowstone flow with rounded edges was also analyzed. The zircons were epoxy-mounted and polished to expose grain interiors. Larger size fractions were mounted separately so that smaller grains would not be overly thinned during polishing.

The zircons were analyzed for their ^{238}U–^{232}Th–^{230}Th compositions using the UCLA CAMECA ims 1270 ion microprobe following the analytical techniques described by Reid et al. (1997). Analytical conditions are given in the caption for Table 1. Repeated analysis of ancient AS3 and 91500 zircon standards ($n = 33$) yield a weighted mean $(^{230}Th)/(^{238}U)$ of 1.01 ± 0.01 (1σ) and replicate analysis of grains during multiple sessions yielded results within analytical error of each other. A few grains that are in, or close to, ^{238}U–^{230}Th secular equilibrium were reanalyzed by ion microprobe U–Pb isotope analysis following the analytical techniques of Dalrymple et al. (1999). Whole-rock vitrophyres, as well as a bulk zircon separate from the Gibbon River flow, were analyzed for U and Th isotopes by thermal ionization mass spectrometry (TIMS) at UCLA. These whole-rock data were used to constrain the initial ^{230}Th abundances of the zircons.

To establish the geochemical variations within the successive CPM lavas, pristine glasses from eight lavas spanning the entire eruptive episode were analyzed for their Sr and Nd isotopic composition by TIMS. A whole-rock sample of the Scaup Lake flow was also analyzed. Rb and Sr concentrations of the glasses and whole rock were obtained by isotope dilution-TIMS.

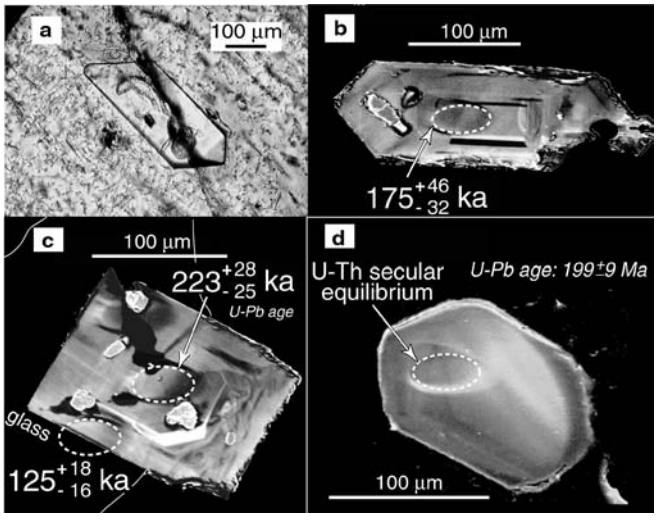

Fig. 2 **A** Photomicrograph of a typical euhedral CPM zircon in Solfatara Plateau flow vitrophyre. Irregular blebs in the grain are melt inclusions. **B** Cathodoluminescence (CL) image of euhedral zircon from West Yellowstone flow. Right side of grain and edges were broken during the polishing process. Faint internal zoning is euhedral with no significant resorption boundaries (cf. Robinson and Miller 1999). Age determined by ^{238}U–^{230}Th disequilibrium analysis. **C** CL image of West Yellowstone zircon. Ion-probe spot on edge of grain partly intersects adhering glass and yields a ^{238}U–^{230}Th age identical to the K–Ar eruption age; the glass has no effect on the age. Unlike the grain in **B**, the core is surrounded by an area of convolute zoning suggesting resorption and yields a distinctly older ^{238}U–^{206}Pb age. **D** CL image of rare rounded zircon from West Yellowstone flow with resorbed core in ^{238}U–^{230}Th secular equilibrium (U–Pb age of 199 ± 9 Ma)

Results

U–Th isotope results for the zircons and host vitrophyres are given in Table 1. Model ages obtained from these data (Table 1, Fig. 3) are those of zircon crystallization (Reid et al. 1997). Most of the zircon ages span the range from that of their respective eruptions to ~200 ka and, as with characteristics such as clarity or inclusion concentration, do not correlate with U/Th. In the case of the West Yellowstone flow, the cores of the larger (125–300 μm) grains yield older ages and have lower U/Th than their rims (Fig. 3). Growth zones imaged by cathodoluminescence are euhedral in nearly all of the analyzed zircons, with little to no evidence of resorption (Fig. 2). The exceptions are the cores of West Yellowstone grains that yield ages > 200 ka, which are associated with disturbed zoning that is suggestive of resorption. A few grains that gave ^{238}U–^{230}Th close to or within error of secular equilibrium yielded ^{207}Pb-corrected ^{238}U–^{206}Pb isotope ages between ~200–350 ka and two older ages of 770 ± 109 ka and 1192 ± 88 ka (Table 2). The rounded grain from the West Yellowstone flow (Fig. 2d) has an unusually high U/Th and yields a concordant age of 199 ± 9 Ma (1σ).

Weighted mean zircon ages for the CPM rhyolites and their mean squared weighted deviates (MSWD) are given in Fig. 3. The U–Th model age for the bulk zircon separate is slightly younger than the weighted mean of the ion probe analyses for the Gibbon River flow (118 ± 4 ka versus 136^{+16}_{-14}ka, MSWD = 1.1). Zircon age distributions for the Dry Creek, Solfatara Plateau, and Gibbon River flows are statistically consistent with a single episode of zircon crystallization, but the analytical uncertainties do not preclude a more distributed age population. The MSWD of the zircon ages for the Pitchstone Plateau and West Yellowstone flows fall outside the 95% confidence interval expected for a single age population, even after grains with ages ≥250 ka or resorbed cores are excluded, and the distribution of ages suggests that nucleation and crystallization continued up to the time of eruption. Despite this possible evidence for a protracted crystallization history, except for a few old grains, the overlap is limited between the episodes of

Table 1 U–Th isotope data for Central Plateau member lavas and zircons

Sample	(^{230}Th)/(^{232}Th)	±	(^{238}U)/(^{232}Th)	±	Model age[a] (ka)	+	–
Vitrophyres and zircon separate (TIMS)[b]							
YCV04	0.759	0.002	0.741	0.001	NA	NA	NA
YCV09	0.852	0.003	0.745	0.001	NA	NA	NA
YCV14	0.765	0.003	0.737	0.001	NA	NA.	NA
YCV12	0.779	0.002	0.751	0.001	NA	NA	NA
YCV17	0.724	0.002	0.642	0.001	NA	NA	NA
YCV17Zr1 (bulk zircon separate)	4.57	0.04	6.45	0.04	118	4	4
Zircons (ion microprobe)[c]							
Solfatara Plateau flow (YCV04) 2.5 km east of Virginia Meadows							
r8g3s1	4.85	0.62	5.42	0.02	226	–	79
r7g2s1	5.34	0.40	6.33	0.02	188	59	38
r8g6s1	4.52	0.21	5.61	0.02	162	25	20
r8g5s1	4.74	0.36	6.06	0.14	150	48	32
r9g4s1	3.96	0.32	5.12	0.02	143	37	27
r8g1s1	5.33	0.46	6.93	0.03	146	39	28
r8g1s2	3.77	0.27	5.00	0.06	134	33	25
r9g8s1	4.09	0.13	4.72	0.02	199	30	23
r8g10s1	4.36	0.13	5.30	0.02	171	18	16
r8g8s1	4.62	0.23	5.83	0.02	155	25	20
r7g4s1	4.10	0.11	4.83	0.02	185	20	17
r7g5s1	3.77	0.13	4.66	0.02	160	20	16
r9g2s1	4.08	0.27	5.79	0.02	117	20	17
r9g9s1	3.89	0.28	4.96	0.01	148	34	26
r9g1s1	6.05	0.63	7.18	0.03	188	93	49
r8g9s1	3.85	0.18	3.95	0.01	359	–	104
r8g7s1	2.39	0.03	2.80	0.00	171	10	9
r6g2s1	3.96	0.46	5.16	0.01	141	54	36
West Yellowstone flow (YCV09) 1.5 km north of Mystic Falls							
r12g2s1	4.25	0.19	5.21	0.01	156	23	19
r11g1s1	4.59	0.18	5.63	0.01	159	20	17
r8g8s1	3.34	0.13	4.50	0.01	118	12	11
r9g9s1	4.76	0.23	5.41	0.01	199	43	30
r8g4s1	5.35	0.25	6.40	0.01	173	28	22
r8g6s1	4.11	0.18	5.26	0.01	139	17	15
r8g10s1	17.36	0.48	17.32	0.02	611	–	242
BG_r3g8s1r	3.90	0.18	4.14	0.01	247	81	46
BG_r3g8s2c	4.38	0.48	5.25	0.02	166	78	45
BG_r3g7s1r	3.74	0.25	4.24	0.01	192	65	40
BG_r3g6s1r	4.07	0.15	4.57	0.01	201	32	25
BG_r3g5s1c	3.94	0.25	4.61	0.01	175	46	32
BG_r3g10s1r	4.58	0.28	5.70	0.01	153	30	23
BG_r3g10s2c	4.08	0.12	4.31	0.01	256	53	36
BG_r3g4s1r	3.56	0.19	4.72	0.01	125	18	16
BG_r3g4s2c	4.46	0.21	4.50	0.01	351	–	99
BG_r3g3s1r	5.10	0.32	5.78	0.01	202	60	38
BG_r3g7s2c	3.20	0.15	3.78	0.01	163	30	23
BG_r3g7s3r	4.37	0.24	6.03	0.01	120	17	15
BG_r3g7s4c	4.13	0.22	4.79	0.01	181	39	29
Dry Creek flow (YCV14) 2.5 km east of Norris Pass							
r4g3s1	3.42	0.18	4.07	0.02	175	38	28
r4g2s1	2.79	0.14	3.46	0.07	149	36	26
r5g5s1	3.00	0.20	3.84	0.01	139	31	24
r6g2s1	4.55	0.28	4.82	0.01	288	–	76
r6g2s1	3.78	0.31	4.50	0.01	176	63	39
r7g1s1	4.00	0.28	4.59	0.01	200	70	42
r7g5s1	3.52	0.20	4.30	0.01	162	35	26
r6g5s1	3.24	0.22	4.10	0.01	146	34	26
r7g2s1	3.46	0.18	4.24	0.02	160	30	23
r4g1s1	3.22	0.28	4.21	0.02	134	37	27
r4g4s1	3.72	0.33	4.62	0.02	157	53	35
r6g3s1	3.00	0.22	3.43	0.04	193	91	48
Pitchstone Plateau flow (YCV12) 5 km east of Phantom Fumarole							
r7g2s1	3.05	0.10	4.73	0.01	93	7	7
r5g9s3	5.02	0.24	5.22	0.02	325	–	83
r5g9s2	3.66	0.17	5.16	0.01	116	13	12
r4g2s1	3.83	0.17	5.62	0.01	108	12	10
r6g6s1	6.03	0.30	6.17	0.01	383	–	117

Table 1 (Contd.)

Sample	$(^{230}Th)/(^{232}Th)$	±	$(^{238}U)/(^{232}Th)$	±	Model age[a] (ka)	+	–
r7g10s1	3.31	0.13	5.02	0.01	99	9	8
r3g8s1	3.83	0.15	5.05	0.01	136	15	13
r7g1s1	4.39	0.16	4.85	0.01	233	47	32
r7g3s1	3.41	0.21	5.71	0.01	83	11	10
r6g7s1	3.18	0.17	5.34	0.01	81	9	8
r6g9s1	3.70	0.23	5.80	0.02	95	13	12
r6g1s1	2.17	0.14	3.43	0.01	80	14	12
r3g3s1	4.33	0.30	6.00	0.01	124	22	18
r4g5s1	1.64	0.10	2.14	0.07	106	37	25
r6g2s1	1.74	0.07	2.61	0.02	80	12	10
r3g9s1	3.65	0.17	4.90	0.01	128	17	15
r4g4s1	3.78	0.22	5.48	0.01	110	16	14
Gibbon River flow (YCV17) Cliff on east side of Gibbon Canyon							
r3g2s1	3.20	0.45	4.92	0.01	94	32	25
r3g1s2	4.11	0.43	4.80	0.06	183	107	52
r3g4s1	3.70	0.21	4.86	0.01	133	21	18
r3g5s1	4.11	0.25	4.92	0.02	171	40	29
r3g9s1c	3.83	0.32	5.81	0.02	101	19	16
r3g9s2r	3.33	0.26	4.72	0.02	112	23	19
r3g6s1	4.92	0.22	6.16	0.02	156	22	18
r4g2s1r	4.85	0.46	6.57	0.02	130	34	25
r4g2s2c	4.53	0.43	5.92	0.10	140	47	32
r3g7s1r	4.57	0.37	6.48	0.02	117	24	19
r3g7s2c	2.78	0.12	3.68	0.07	123	21	17
r4g9s1	6.61	0.53	7.07	0.15	269	–	85
r6g12s1	4.20	0.44	5.60	0.33	132	73	39
r4g10s1	5.22	0.23	6.81	0.02	143	17	15
r3g1s3	3.29	0.26	4.21	0.01	139	34	26

[a]Model ages calculated using zircon–vitrophyre isochrons. Decay constants used for age calculations: λ_{230}: 9.1577×10^{-6} year^{-1}; λ_{232}: 4.9475×10^{-11} year^{-1}; λ_{238}: 1.55125×10^{-10} year^{-1}. *Dashes* indicate secular equilibrium. Uncertainties on ratios and model ages are 1σ

[b]Analytical details for vitrophyre U and Th TIMS analyses are the same as described by Bohrson and Reid (1998); reproducibility ~1%

[c]Analytical conditions during ion microprobe analyses: mass resolving power ~6,000, 25×50 μm spot 20–80 nA primary $^{16}O^-$ beam. Isotopes measured as $^{230}Th^{16}O^+$, $^{238}U^{16}O^+$, and $^{232}Th^{16}O^+$. Data corrected for ~0.04 cps background. Relative sensitivity factor used for conversion of oxide to metal ratios was determined from Th/U measured in standards for each analytical session; average factor: 1.09. From left to right, ion probe sample numbers denote grain mount row, grain, spot number, and core or rim analysis

zircon crystallization in the Pitchstone Plateau flow and those of the older Dry Creek, West Yellowstone, and Solfatara Plateau flows.

Sr and Nd isotope compositions of the CPM glasses are given in Table 2. Both Sr and Nd isotope compositions generally become more radiogenic with decreasing eruption age (Fig. 4); those of the earliest CPM lavas overlap that of the somewhat older Scaup Lake flow as well as the least-evolved composition of the Lava Creek Tuff (cf. Hildreth et al. 1991), but are distinct from the ~500 ka UBM lavas. Rb and Sr concentrations of CPM glasses are similar to previously reported values (cf. Halliday et al. 1991) and Rb/Sr also increases with decreasing eruption age (Table 3, Fig. 5).

Evolution of magma beneath Yellowstone caldera

Zircon constraints on magma genesis of the CPM lavas

Ages obtained from ^{238}U–^{230}Th disequilibria reflect crystallization and not magmatic re-equilibration of zircon (Reid et al. 1997). Consequently, zircon ages represent the attainment by the magma of the thermochemical conditions for zircon saturation and, thus, can be used to track the crystallization history and kinship of rhyolites (Reid et al. 1997; Brown and Fletcher 1999; Lowenstern et al. 2000). Zircon saturation temperatures for the CPM lavas are ~850–900 °C, and ~800 °C for the extracaldera Gibbon River flow, based on experimental constraints on zircon saturation in rhyolitic magma (Watson and Harrison 1983), whereas the presence of accessory allanite phenocrysts in the West Yellowstone and Pitchstone Plateau flows suggests cooling to ~800 °C (cf. Chesner and Ettlinger 1989). Therefore, the zircon ages relate to magmatic evolution of the CPM rhyolites in this temperature window.

Three important results from the record of zircon crystallization in the CPM rhyolites are the following. First, the majority of zircon ages fall within the eruptive episode associated with the CPM eruptions and, therefore, are young and distinct relative to the duration of rhyolitic magmatism associated with Yellowstone and even with respect to the duration of post-collapse magmatism (Fig. 3). Second, most of the zircons crystallized

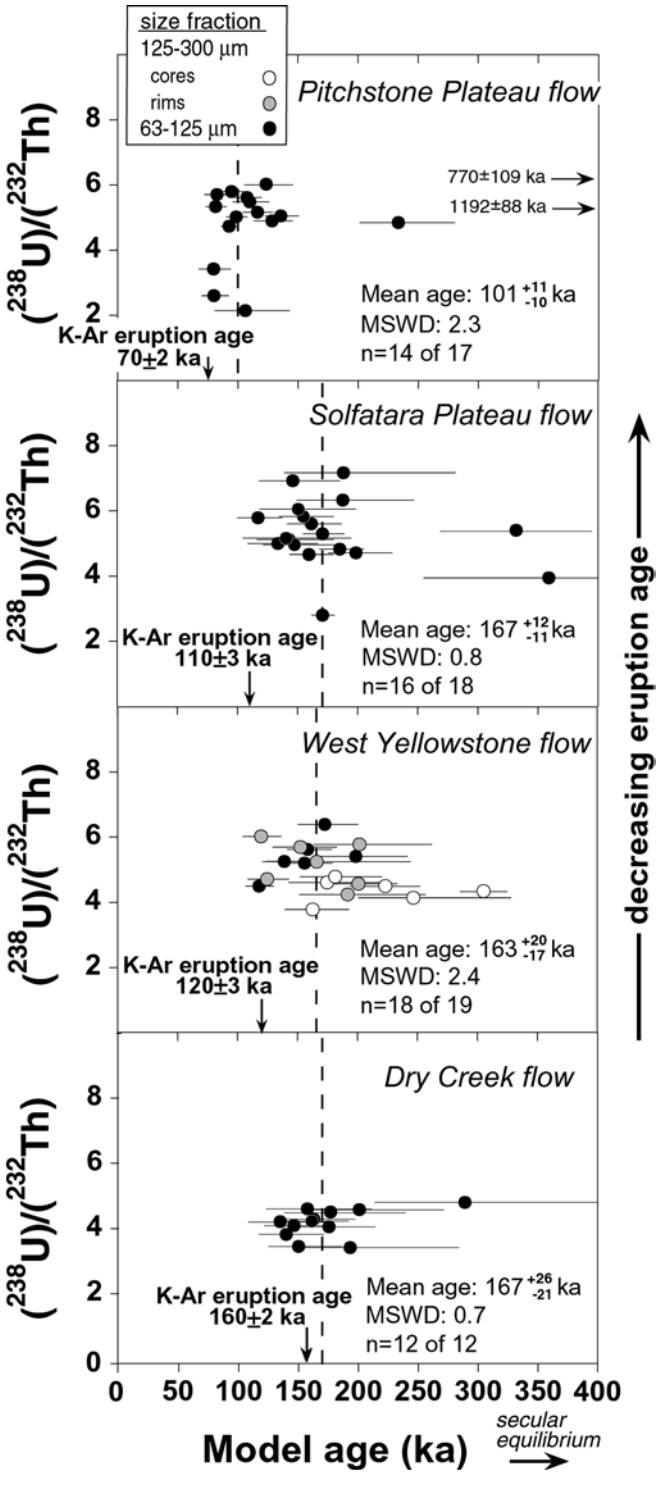

Fig. 3 ^{238}U–^{232}Th activity ratio versus model age diagrams showing results for zircons from Central Plateau Member lavas. *Arrows* delimit K–Ar eruption ages and are listed with 1σ uncertainties; mean zircon ages from each lava (discussed in text) are shown by *vertical line*; uncertainties (95% confidence) on mean ages are calculated according to Ludwig and Titterington (1994). Uncertainties shown for individual model ages are 1σ. *Horizontal arrows* point towards ^{238}U–^{206}Pb ages >400 ka

within tens of thousand years of their K–Ar ages for eruption. Third, there is considerable overlap between the zircon age populations of most of the CPM rhyolites, with the notable exception to this being the distinctly younger zircon population of the youngest, most-evolved Pitchstone Plateau flow. These observations are intriguing because they imply an effective crystal storage time of tens of thousands of years for some, but not all temporally and spatially associated rhyolites, magmas which are, in turn, associated with a volcanic system characterized by secular isotopic and chemical trends that extend over time scales of hundreds of thousands of years (cf. Hildreth et al. 1984, 1991).

Some uncertainty about the duration of CPM eruptive activity (160–70 ka), and especially the extent to which zircon crystallization preceded eruption, could result from inaccuracy of the K–Ar-derived eruption ages. Inaccuracies would likely be due to incomplete degassing of sanidine during Ar-isotope analysis (Obradovich 1992), which would make the K–Ar ages younger than the true age of eruption and thus appear to increase the difference between the zircon mean ages and eruption. Nonetheless, recent $^{40}Ar/^{39}Ar$ dating of sanidine from the samples corroborates the K–Ar eruption ages (T.A. Dallegge et al., in preparation), as does the clustering of the youngest zircon ages about the K–Ar age for each lava.

The younger model age for the bulk zircon separate compared with the weighted mean ion probe age for the Gibbon River flow zircons, and the similarity between the U/Th of the separate and the zircon rims, is expected of bulk zircon analyses because U and Th tends to be concentrated in the rims of zircon crystals (cf. Charlier and Zellmer 2000). Even so, the absolute values of both sets of zircon ages are subject to uncertainties about the extent to which the initial ^{230}Th of the zircons can be accurately constrained by assuming that the isotopic compositions of the vitrophyres reflect those of the zircon hosts at the time of crystallization. This is noteworthy because the vitrophyres contain variable and significant ^{230}Th excesses that, if characteristic of the magmas, would have been even more pronounced at the time of crystallization, given the antiquity of the zircons. Hydrothermal alteration could cause disequilibrium. However, the vitrophyres are very fresh and alteration in the Yellowstone system would likely cause ^{238}U, not ^{230}Th, excess (cf. Sturchio et al. 1987). Pronounced ^{230}Th excesses could reflect large degrees of U–Th fractionation during initial melt generation (Condomines et al. 1988), accessory mineral fractionation (LaTourette et al. 1991), and/or periodic recharge by magmas (Hughes and Hawkesworth 1999), and have been reported for evolved rhyolites from East Africa (Black et al. 1997, 1998; Lowenstern et al. 2001). Allowing for the range of Th-isotope compositions and U/Th measured for the CPM vitrophyres as a model for the evolving magma system in which the zircons crystallized would introduce an uncertainty to the U–Th zircon ages of $\leq 10\%$ for ages <200 ka and $\leq 15\%$ for ages >200 ka. Hence, the

Table 2 U–Pb isotope results for CPM zircons

Sample	$^{238}U/^{206}Pb$[a]	±	$^{207}Pb/^{206}Pb$	±	$^{238}U/^{206}Pb$ age[a] (ka)	±
YCV09BGr3g4s5 at 2	16,594	940	0.384	0.032	223	27
YCV09BGr3g10s3 at 2	17,638	773	0.151	0.016	306	21
YCV04r8g3s2 at 1	12,831	1,168	0.306	0.048	332	58
YCV12r5g9s3 at 2	4,620	300	0.135	0.006	1,192	88
YCV12r6g6s2 at 1	1,083	35	0.775	0.012	770	109
YCV09r8g10s2 at 1	31.8	1.4	0.051	0.000	199×10^3	9×10^3

[a]Adjusted for initial ^{238}U–^{230}Th disequilibrium according to Shärer (1984) and model ages calculated using initial $^{207}Pb/^{206}Pb$ of 0.9 characteristic of CPM lavas (cf. Doe et al. 1982; Vazquez and Reid unpublished data). Analytical techniques and conditions as in Dalrymple et al. (1999). Uncertainties are 1σ

zircon ages are robust, even after allowing for the most significant possible uncertainties.

Evidence for a common magma heritage for the CPM lavas

If the CPM rhyolites were variably aged, but otherwise unrelated batches of rhyolite, like those of the post-collapse rhyolite lavas of Valles (Spell et al. 1993) and Taupo calderas (Sutton et al. 2000), they might be expected to exhibit incoherent chemical and/or isotopic characteristics and have no crystal "memory" of each other. In contrast, the CPM zircon ages are comparably young and, except for the youngest eruption, essentially identical. The Sr and Nd isotope compositions of the CPM lavas are also relatively similar and distinct when compared with other Yellowstone-related rhyolites (Fig. 4). Progressively increasing $^{87}Sr/^{86}Sr$ can be explained by the combined effects of ^{87}Rb decay in the high Rb/Sr magmas over the ~130,000-year interval of zircon crystallization coupled with minor contamination. The slight increase in the Nd-isotope compositions of the CPM lavas over their eruptive interval could, like increasing $\delta^{18}O$ values (Hildreth et al. 1984), reflect inputs of rhyolitic magma from lower in the subcaldera system and/or contamination from wall rock melts. The high and progressively increasing Rb/Sr ratios for successively erupted CPM glasses (Fig. 5) are indicative of increasing differentiation due to >40% fractionation of the sanidine-dominated mineralogy (cf. Halliday et al. 1991), not even including the more extreme fractionation required for the Pitchstone Plateau flow. Progressive changes in trace element concentrations (e.g., Ba, Y, Ce) and mineral compositions (Leeman and Phelps 1981; Christiansen 1984a, 2001; Hildreth et al. 1984, 1991; Bindeman and Valley 2001) are also consistent with at least 40% fractionation. Notably, zircon fractionation (~0.07%) may have differentially affected only the youngest CPM rhyolite, as evidenced by the fact that the Zr/Hf ratios of CPM lavas are relatively constant except for the Pitchstone Plateau flow, which has a lower ratio (Hildreth et al. 1991). Considered together with the volume (10–100 km^3 per flow) and wide areal extent spanned by coeval CPM vents, these features are consistent with tapping of a large, evolving, but otherwise common rhyolitic CPM magma reservoir (cf. Bacon 1985; Duffield and Ruiz 1992; Justet and Spell 2001).

If the CPM lavas erupted from a long-standing rhyolitic reservoir that reached zircon saturation early in its evolution, they should remember a protracted history of zircon crystallization. Zircon is an early-crystallizing and persistent mineral in silicic magmas and formed in the bodies of rhyolitic magma that erupted the Lava Creek Tuff and UBM. Loss of the oldest zircons stochastically due to gravitational settling is unlikely to be significant over time scales of hundreds of thousands of years (Reid et al. 1997) because of the typically small size of zircon and high viscosity of rhyolite melt, even though it can be appreciable for coexisting major phases. Specific to the main body of the CPM rhyolite, evidence for zircon retention is provided by progressively increasing Zr concentrations in lavas erupted between 160 and 110 ka (data of Leeman and Phelps 1981; Hildreth

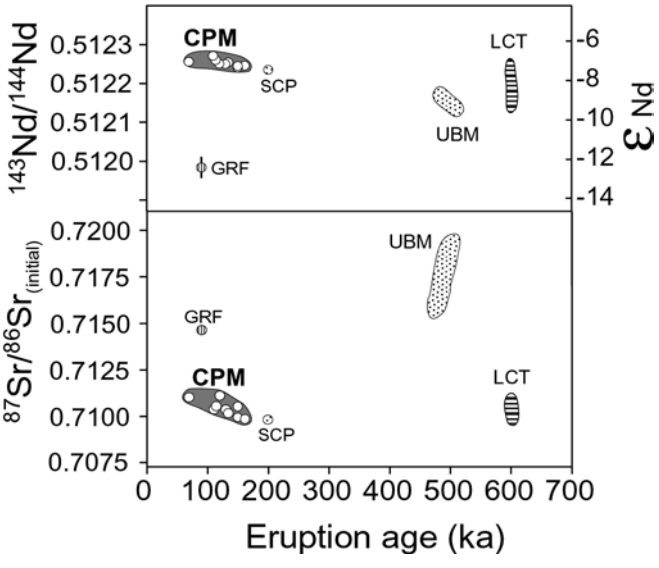

Fig. 4 Sr and Nd isotopic compositions of Yellowstone caldera lavas showing similarity of the CPM lavas and their distinctiveness relative to the other caldera rhyolites, particularly the UBM lavas. Note general trend of increasing $^{87}Sr/^{86}Sr$ with decreasing eruption age in the CPM lavas and the similarity of the Scaup Lake flow to the earliest of these (see text for discussion). *CPM* Central Plateau Member; *UBM* Upper Basin Member; *LCT* Lava Creek Tuff; *SCP* Scaup Lake flow; *GRF* Gibbon River flow (extracaldera). Data for UBM, LCT, and GRF are from Hildreth et al. (1991)

Table 3 Rb, Sr, and Nd isotopic composition of Central Plateau Member glasses. Glass samples represent ~200 mg of hand picked and pristine obsidian. Analytical and chemical techniques as in Wolff et al. (1999). Rb and Sr concentrations in ppm and determined by isotope dilution TIMS; reproducibility < 1%. Sr and Nd isotope ratios were measured by TIMS in dynamic mode and normalized to $^{86}Sr/^{88}Sr = 0.1194$ and $^{146}Nd/^{144}Nd = 0.7219$. Replicate analyses of NBS987 and La Jolla standards yield weighted mean $^{87}Sr/^{86}Sr$ of 0.710240 ± 13 ($n = 8$) and $^{143}Nd/^{144}Nd$ of 0.511843 ± 12 ($n = 4$), respectively; ratio uncertainties are 2σ. Sr and Nd blanks are insignificant

Lava	Eruption age[a] (ka)	Rb	Sr	Rb/Sr	$^{87}Rb/^{86}Sr$	$^{87}Sr/^{86}Sr_{initial}$	$^{143}Nd/^{144}Nd$
Pitchstone Plateau	70 ± 2	202.8	1.47	138	399	0.71101 ± 1	0.512257 ± 8
Solfatara Plateau	110 ± 3	261.7	7.05	37.1	107	0.71116 ± 2	0.512252 ± 8
Hayden Valley	114 ± 11	213.1	2.62	81.4	233	0.71054 ± 1	0.512261 ± 9
West Yellowstone	120 ± 3	236.4	3.88	60.9	174	0.71039 ± 1	0.512271 ± 9
Summit Lake	131 ± 3	178.4	3.03	58.8	170	0.71037 ± 2	0.512250 ± 8
Spring Creek	(150)	135.5	5.00	27.1	77.4	0.71054 ± 1	0.512245 ± 9
Mallard Lake	149 ± 5	162.2	7.57	21.4	61.2	0.70993 ± 1	0.512241 ± 7
Dry Creek	162 ± 2	188.8	8.36	22.6	64.5	0.70987 ± 1	0.512246 ± 9
Scaup Lake[b]	198 ± 8	188.1	68.3	2.76	7.29	0.70993 ± 1	0.512236 ± 6

[a]Eruption ages (1σ) from Obradovich (1992; K–Ar) and Gansecki et al. (1996; Ar/Ar); age of Spring Creek flow is constrained by dated stratigraphy
[b]Whole rock

et al. 1984, 1991; Bindeman and Valley 2001) despite geochemical evidence for fractionation of major phases. Loss of zircon via dissolution associated with volatile flushing or magma ascent is also unlikely given the general insensitivity of zircon solubility in rhyolitic melts to water and halogen content or pressure (Watson and Harrison 1983; Baker et al. 2002). Consequently, the lack of significant age overlap between the CPM zircons and the abundant zircons of the UBM and Lava Creek Tuff magmas (Fig. 6) indicates that the CPM are not derived from a persistent body of rhyolite magma residual to the caldera-forming eruption.

The presence of significant amounts of inherited zircons in early post-caldera (~500 ka) UBM lavas (cf. Fig. 6) led Bindeman and Valley (2000, 2001) and Bindeman et al. (2001) to suggest a general model in which Yellowstone's post-collapse volcanism results from remelting of collapsed wallrock and subcaldera intrusions, similar to more general models of crystal recycling and/or remobilization that have been proposed for silicic magma systems (e.g., Mahood 1990; Sparks et al. 1990; Bacon et al. 2000). However, the youth of the CPM zircons rules out appreciable crystal recycling (Fig. 6). We note that this constraint on the relationship of the CPM lavas to early intrusions is unique: the radiogenic isotope compositions of CPM and Lava Creek Tuff rhyolites are similar enough to otherwise be permissive of derivation of the CPM from remelting of intrusions associated with the Lava Creek Tuff. In order for zircons to be largely dissolved during remobilization of rhyolitic mush, essentially complete remelting (e.g., Watson 1996) and near equal proportions of basalt to rhyolite (cf. Snyder 2000) would be required. This would likely result in significant hybridization (cf. Sparks and Marshall 1986), yet there is no direct evidence for mixing of CPM magma with more mafic magma, such as disequilibrium mineral assemblages, mafic enclaves, or intermittent eruption of less evolved whole-rock compositions. Only the few CPM zircons that have cores > 200 ka and, therefore, pre-date eruption of the CPM, are bounded by the disrupted growth patterns expected of remelting (cf. Robinson and Miller 1999).

Instead of sporadic remobilization of subcaldera intrusions, the youthful crystallization ages for the majority of the CPM zircons suggest that the lavas are the

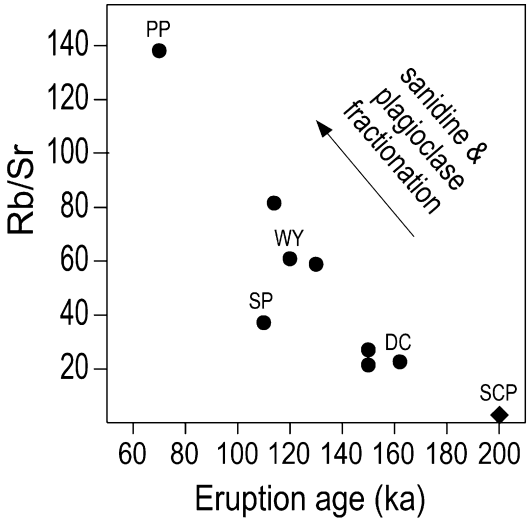

Fig. 5 Temporal Rb/Sr variation of glasses from CPM lavas (*dots*) and a Scaup Lake flow whole rock (*diamond*). Crystallinity of the lavas is 10–30%, as with other CPM lavas (Hildreth et al. 1984), and shows no temporal trend. Whole rocks follow a similar trend of progressively increasing Rb/Sr (Hildreth et al. 1991; Bindeman and Valley 2001). The trend is consistent with derivation of the lavas from rhyolitic magma undergoing progressive fractionation involving sanidine and/or plagioclase. Total variation in the CPM rhyolites can be produced by a minimum of 40% fractionation (cf. Halliday et al. 1991) of the sanidine + quartz + cpx ± fayalite ± plagioclase assemblage typical of CPM lavas. *PP* Pitchstone Plateau flow; *WY* West Yellowstone flow; *SP* Solfatara Plateau flow; *DC* Dry Creek flow; *SCP* Scaup Lake flow

product of a period of rhyolite differentiation that largely post-dates the Lava Creek Tuff. Furthermore, it appears that a second, superimposed pulse of differentiation is required for the distinctly younger zircon population of the Pitchstone Plateau flow magma. Punctuated changes in accessory-mineral-sensitive trace-element ratios, such as the decrease in Zr/Hf that characterizes the Pitchstone Plateau flow, are consistent with episodic crystal-melt separation from mushy magma (Johnson et al. 1989). Effective crystal-melt separation can occur relatively quickly at shallow depths by gas-driven filter pressing of mushy magma (Sisson and Bacon 1999) and/or melt channelization through fractures (Miller and Mittlefehldt 1984; Trial and Spera 1990; Mahood and Cornejo 1992); such mechanisms may have extracted interstitial rhyolitic melt from a mush column below the caldera to produce melt-rich magma reservoirs. Accordingly, the onset of zircon crystallization in individual CPM lavas would correspond to episodes of effective crystal-melt separation at ~200 ka and at ~125 ka.

Magmachronology of rhyolite at Yellowstone caldera

The results presented here combined with those from previous studies delimit the evolutionary history of rhyolitic magma erupted from Yellowstone caldera (Fig. 7). Based on recent U–Pb dating of zircons, generation of the rhyolitic magma responsible for the voluminous Lava Creek Tuff likely occurred < 100,000 years prior to eruption at 0.64 Ma (Bindeman et al. 2001). Approximately 150,000 years after the caldera-

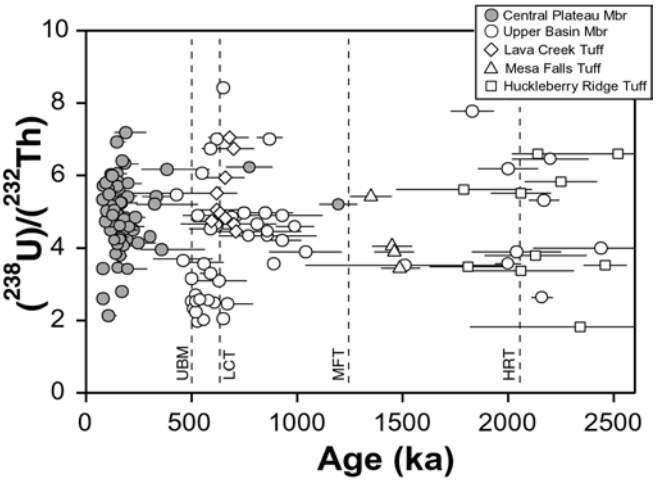

Fig. 6 Zircon ages for Yellowstone Plateau volcanic field rhyolites. The population of CPM zircons is distinct from those in rhyolites erupted earlier from the magmatic system and, thus, is not inherited. *Vertical dashed lines* delimit important episodes of volcanism in the Yellowstone system (Hildreth et al. 1984; Gansecki et al. 1996; Lanphere et al. 2002) at ~500 ka (UBM; ~40–70 km^3), ~640 ka (LCT; 1,000 km^3), ~1,300 ka (MFT: Mesa Falls Tuff; 280 km^3), and ~2,100 ka (HRT: Huckleberry Ridge Tuff; 2,800 km^3). Zircon ages besides those for CPM lavas are from U–Pb analyses by Bindeman et al. (2001)

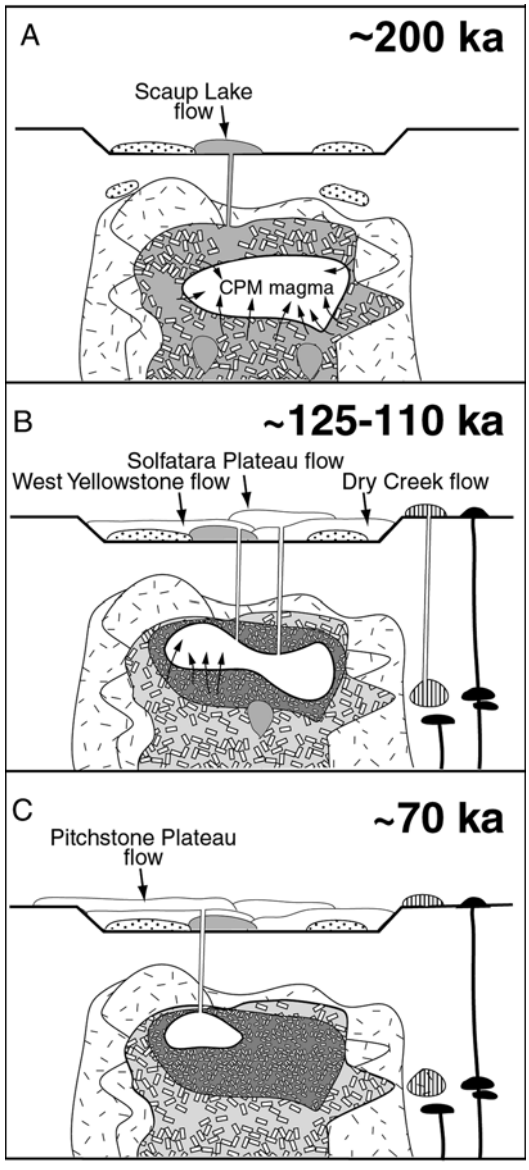

Fig. 7A, B Evolution of late Pleistocene rhyolitic magma beneath Yellowstone caldera. **A** Fractionation/generation of early CPM magma due to effective crystal-melt separation from a hybridized and less-evolved subcaldera system of mushy magma at ~200 ka. At about the same time, the Scaup Lake flow erupts, likely from the same mushy system. Approximately 500 ka UBM magmas produced by isolated wallrock melting are denoted by *dotted pattern*. **B** Differentiation of the CPM reservoir produces a suite of progressively more-evolved rhyolite compositions that are erupted between ~160 and 110 ka. Superimposed on the continuous "background" fractionation of major phases in the CPM magma is effective crystal-melt fractionation at ~125 ka, possibly occurring in a more-mushy and/or isolated portion of the crystallizing reservoir. Sustaining thermal energy is provided by cooling of hotspot-related mafic magmas deeper in the system, as well as inputs of silicic magma from lower in the subcaldera system that mix to a limited extent with CPM magma. Outside of the subcaldera system, localized melting of wall rock produces isotopically distinct magmas that are erupted as extracaldera rhyolites alongside basaltic lavas. **C** Eruption of Pitchstone Plateau flow magma at ~70 ka after 40,000–50,000 years of storage and crystallization

forming eruption, anomalously low $\delta^{18}O$ UBM magmas with distinctive Sr- and Nd-isotope compositions (Fig. 4) were produced by either melting of hydrothermally altered wall rock due to heating by a "hot" subcaldera reservoir (Bindeman and Valley 2000), or contamination of residual subcaldera rhyolite (Hildreth et al. 1984, 1991). This magmatism was followed by an eruptive hiatus between ~500 and ~200 ka, but the presence of ~200- to ~350 ka ages in CPM zircons reveal that silicic magmas were crystallizing in the subcaldera system (Fig. 6). By ~200 ka, magma with Sr- and Nd-isotope compositions (Fig. 4), as well as $\delta^{18}O$ values (Hildreth et al. 1984; Gansecki et al. 1996), essentially identical to the early CPM lavas was present beneath the caldera, as evidenced by eruption at that time of the CPM-like Scaup Lake flow (Fig. 4). At about that same time, extensive crystal-melt fractionation of mushy subcaldera magma, from which the older CPM zircon cores may have been extracted, gave rise to a voluminous body of high-silica rhyolitic magma from which major phases, but not zircon, fractionated (Fig. 7); the Scaup Lake flow may most closely approximate the composition of the parental mushy magma. Between 160 and 110 ka, nearly all of the CPM rhyolites erupted from this evolving magma reservoir. Another momentous episode of crystal-melt fractionation at ~125 ka produced magma with little zircon-crystal memory of the rhyolitic magmatism that preceded it, possibly due to separation of melt from a mushy and/or isolated portion of the magma reservoir created in the aftermath of removal of large volumes of CPM rhyolite. Storage of this new magma for 40,000–50,000 years allowed new zircons and crystals to grow prior to eruption as the Pitchstone Plateau flow, the youngest rhyolite in Yellowstone caldera.

Time scales of rhyolite magma storage

Besides fingerprinting the CPM magmas as a distinct episode of rhyolite differentiation beneath Yellowstone caldera, the eruption of magmas with similar zircon age populations over a period of ~50,000 years (from 160 to 110 ka) provides evidence for durations of magma storage that are protracted with respect to simple cooling histories. Qualitative evidence for zircon crystallization at least tens of thousands of years before eruption is also suggested by the crystal-size distribution in a CPM lava (Bindeman and Valley 2001). A similar time scale of pre-eruptive storage is also implied for the extracaldera Gibbon River flow by the ~40,000 -year difference between its eruption age and the mean age of zircon crystallization, even though the extracaldera lavas at Yellowstone caldera likely represent volumetrically small and transient batches of rhyolite (e.g., Hildreth et al. 1984, 1991). If the present-day power output of the Yellowstone caldera system (5,300 MW; Christiansen 1984a) applied during evolution of the CPM reservoir and was derived solely from closed-system cooling of the resident magma, then a volume of rhyolite like that erupted would solidify in $<10{,}000$ years (cf. Hawkesworth et al. 2000); even if the erupted volume represents only 10% of the resident reservoir (e.g., Smith 1979; Crisp 1984), the solidification time (ca. 50,000 years) would still be less than the ~90,000-years duration of CPM eruptions from the evolving magma reservoir. Thus, besides providing the thermal energy required to generate Yellowstone rhyolites (Christiansen 2001), it appears that a significant fraction of the power output may have been provided by the thermal inputs associated with cooling of hotspot-related basaltic magma. Basaltic magmatism contemporaneous with evolution of the CPM reservoir is evidenced by eruption of coeval extracaldera basalts (Christiansen 2001). Proximity to mafic magmas and/or thermal coupling to the adjacent subcaldera reservoir, even possibly as an apophysis, probably also facilitated storage of the presumably small batch of Gibbon River flow magma.

The perspective that the CPM rhyolites provide on the evolution of silicic magma reservoirs is unique. Like caldera-forming ignimbrites, they sample a voluminous magma reservoir; like rare suites of rhyolite domes and lavas, they probe a differentiating reservoir. Had evolution of the CPM magmas been terminated by a single eruptive episode, as for ignimbrite-forming eruptions, then the zircon ages might have ranged to $>200{,}000$ years before eruption, but the persistence of the reservoir would be represented by the ages that cluster $<130{,}000$ years before eruption (cf. Fig. 6). If erupted from a reservoir that was compositionally zoned by episodic differentiation via effective crystal-melt fractionation (e.g., Davies and Halliday 1998), our results suggest that the compositional zones might be characterized by distinct zircon age distributions. The relative ages of these hypothetical zones, as well as the degree of age overlap between their zircons, would likely depend on the extent to which differentiation occurs by expulsion of melt from a mushy magma, as inferred for the CPM rhyolites, rather than by crystal settling or sidewall crystallization.

The average pre-eruptive zircon crystallization ages for individual CPM rhyolites (up to ca. 60,000 years, excluding resorbed and inherited grains), as well as collectively (~130,000 years), are similar to those estimated for Member A of the Lava Creek Tuff (Bindeman et al. 2001). These crystal residence ages for voluminous Yellowstone rhyolites are intermediate between those estimated for rhyolites associated with calderas that have total eruptive volumes comparable to that of Yellowstone caldera. They are considerably shorter than the pre-eruptive crystallization ages and/or storage time scales for apparently related batches of small volume, pre- and post-collapse rhyolites associated with Long Valley caldera (hundreds of thousands of years; e.g., Davies et al. 1994; Reid et al. 1997; Heumann et al. 2002), but comparable to the maximum storage estimate ($<100{,}000$ years; Reid and Coath 2000) for the associated voluminous caldera-forming rhyolite (Bishop

Tuff). They are also similar to those estimated for batches of post-collapse rhyolites at Valles caldera that apparently resided tens of thousands of years (Spell et al. 1993); unlike the CPM rhyolites, these Valles rhyolites are unrelated to one another. On the other hand, even though caldera-forming rhyolite from Whakamaru caldera resided for at least 200,000 years (Brown and Fletcher 1999), post-collapse 7rhyolite at adjacent Taupo caldera apparently resided only hundreds to thousands of years (Sutton et al. 2000). Given the evidence from the CPM for episodic production of rhyolite and the likelihood that factors such as local tectonics affect the probability of magma escape from reservoirs (e.g., Bacon 1982), the variable apparent storage times of the large- and small-volume rhyolites erupted from long-lived caldera systems suggest that the chemical and physical evolution of rhyolite may be strongly path-dependent.

Conclusions

Despite chemical and isotopic affinities that suggest the evolution of a long-lived and coherent body of rhyolite beneath Yellowstone caldera (e.g., Hildreth et al. 1984, 1991), the voluminous CPM rhyolites do not represent residual magma from a long-standing magma chamber or remobilization of residual crystals left over from the caldera-forming magma, nor do they represent remelting of wall rock (e.g., Bindeman and Valley 2001). Rather, they represent eruptions from a new magma reservoir that, based on the geochemistry of its magmas and the age distribution of its zircons, persisted and evolved for $>100{,}000$ years. Furthermore, the CPM lavas demonstrate that successive eruptions from an evolving rhyolitic magma reservoir may have similar zircon crystal populations whereas others may lack a significant zircon memory of the less differentiated magmas to which they may be geochemically related. Segregation and accumulation of the voluminous batches of high-silica rhyolite by effective crystal-melt separation erased the zircon memory of earlier crystallization and occurred episodically within tens of thousands of years of eruption.

Acknowledgements We thank Kari Cooper and Justin Simon for helpful discussions, Chris Coath, Axel Schmitt, and Marty Grove for assistance with the ion probe, and Jeremy Boyce for able field assistance. We are also grateful to Charlie Bacon and Jake Lowenstern for thoughtful reviews that helped to improve this paper. This work was supported by a Geological Society of America Lipman Research Award to Vazquez and National Science Foundation grants EAR-9706519 and EAR-0003601 to Reid. The UCLA ion microprobe is partially subsidized by a grant from the National Science Foundation Instrumentation and Facilities Program.

References

Bacon CR (1982) Time-predictable bimodal volcanism in the Coso Range, California. Geology 10:65–69

Bacon CR (1985) Implications of silicic vent patterns for the presence of large crustal magma chambers. J Geophys Res 90:11243–11252

Bacon CR, Persing HM, Wooden JL, Ireland TR (2000) Late Pleistocene granodiorite beneath Crater Lake caldera, Oregon, dated by ion microprobe. Geology 28:467–470

Baker DR, Conte AM, Freda C, Ottolini L (2002) The effect of halogens on Zr diffusion and zircon dissolution in hydrous metaluminous granitic melts. Contrib Mineral Petrol 142:666–678

Bindeman IN, Valley JW (2000) Formation of low-^{18}O rhyolites after caldera collapse at Yellowstone, Wyoming, USA. Geology 28:719–722

Bindeman, IN, Valley JW (2001) Low-^{18}O rhyolites from Yellowstone: magmatic evolution based on analyses of zircons and individual phenocrysts. J Petrol 42:1491–1517

Bindeman IN, Valley JW, Wooden JL, Persing HM, (2001) Post-caldera volcanism: in situ measurement of U–Pb age and oxygen isotope ratio in Pleistocene zircons from Yellowstone caldera. Earth Planet Sci Lett 189:197–206

Black S, Macdonald R, Kelly, MR (1997) Crustal origin for peralkaline rhyolites from Kenya: evidence from U-series disequilibria and Th-isotopes. J Petrol 38:277–297

Black S, Macdonald R, Barreiro BA, Dunkley N, Smith M (1998) Open system alkaline magmatism in northern Kenya: evidence from U-series disequilibria and radiogenic isotopes. Contrib Mineral Petrol 131:364–378

Bohrson WA, Reid MR (1998) Genesis of evolved ocean island magmas by deep- and shallow-level basement recycling, Socorro Island, Mexico: constraints from Th and other isotope signatures. J Petrol 39:995–100

Brown SJA, Fletcher IR (1999) SHRIMP U–Pb dating of the preeruption growth history of zircons from the 340 ka Whakamaru ignimbrite, New Zealand: evidence for >250 ky magma residence times. Geology 27:1035–1038

Charlier BLA, Zellmer G (2000) Some remarks on U–Th mineral ages from igneous rocks with prolonged crystallisation histories. Earth Planet Sci Lett 183:457–469

Chesner CA, Ettlinger AD (1989) Composition of volcanic allanite from the Toba Tuffs, Sumatra, Indonesia. Am Mineral 74:750–758

Christiansen RL (1982) Late Cenozoic volcanism of the Island Park area, Eastern Idaho. In: Bonnichsen B, Breckenridge RM (eds) Cenozoic geology of Idaho. Idaho Bureau Mines Geol 26:345–368

Christiansen RL (1984a) Postcaldera evolution and current activity of the Yellowstone caldera. US Geol Surv Open-File Rep 84-939, pp 743–783

Christiansen RL (1984b) Yellowstone magmatic evolution: its bearing on understanding large-volume explosive volcanism. In: Boyd FR (ed) Explosive volcanism. National Academy of Sciences, Washington, DC, pp 84–95

Christiansen RL (2001) The Quaternary and Pliocene Yellowstone Plateau volcanic field of Wyoming, Idaho, and Montana. US Geol Surv Prof Pap 729-G

Christiansen RL, Blank HR Jr (1972) Volcanic stratigraphy of the Quaternary rhyolite plateau in Yellowstone National Park. US Geol Surv Prof Pap 729-B

Condomines M, Hemond C, Allegre CJ (1988) U–Th–Ra radioactive disequilibria and magmatic processes. Earth Planet Sci Lett 90:243–262

Crisp JA (1984) Rates of magma emplacement and volcanic output. J Volcanol Geotherm Res 20:177–211

Dalrymple GB, Grove M, Lovera OM, Harrison TM, Hulen JB, Lanphere MA (1999) Age and thermal history of the Geysers plutonic complex (felsite unit), Geysers geothermal field, California: a ^{40}Ar/^{39}Ar and U–Pb study. Earth Planet Sci Lett 173:285–298

Davies GR, Halliday AN (1998) Development of the Long Valley rhyolitic magma system: strontium and neodymium isotope evidence from glasses and individual phenocrysts. Geochim Cosmochim Acta 62:3561–3574

Davies GR, Halliday AN, Mahood GA, Hall CM (1994) Isotopic constraints on the production rates, crystallization histories and residence times of pre-caldera silicic magmas, Long Valley, California. Earth Planet Sci Lett 125:17–37

Doe BR, Leeman W, Christiansen, RL, Hedge CE (1982) Lead and strontium isotopes and related trace elements as genetic tracers in the upper Cenozoic rhyolite–basalt association of the Yellowstone Plateau volcanic field. J Geophys Res 87: 4785–4806

Duffield WA, Ruiz J (1992) Compositional gradients in large reservoirs of silicic magma as evidenced by ignimbrites versus Taylor Creek Rhyolite lava domes. Contrib Mineral Petrol 110:192–210

Gansecki CA, Mahood GA, McWilliams MO (1996) $^{40}Ar/^{39}Ar$ geochronology of rhyolites erupted following collapse of the Yellowstone caldera, Yellowstone Plateau volcanic field: implications for crustal contamination. Earth Planet Sci Lett 142:91–107

Halliday AN, Davidson J, Hildreth W, Holden P (1991) Modelling the petrogenesis of high Rb/Sr silicic magmas. Chem Geol 92:107–114

Hawkesworth CJ, Blake S, Evans P, Hughes R, Macdonald R, Thomas LE, Turner S, Zelmer G (2000) Time scales of crystal fractionation in magma chambers – integrating physical, isotopic and geochemical perspectives: J Petrol 41:991–1006

Heumann A, Davies GR, Elliot T (2002) Crystallization history of rhyolites at Long Valley, California, inferred from combined U-series and Rb–Sr isotope systematics. Geochim Cosmochim Acta 66:1821–1837

Hildreth W, Christiansen RL, O'Neil JR (1984) Catastrophic isotopic modification of rhyolitic magma at times of caldera subsidence, Yellowstone Plateau volcanic field. J Geophys Res 89:8339–8369

Hildreth W, Halliday AN, Christiansen RL (1991) Isotopic and chemical evidence concerning the genesis and contamination of basaltic and rhyolitic magma beneath the Yellowstone Plateau volcanic field. J Petrol 32:63–138

Hughes RD, Hawkesworth CJ (1999) The effects of magma replenishment processes on ^{238}U–^{230}Th disequilibrium. Geochim Cosmochim Acta 63:4101–4110

Johnson CM, Czamanske GK, Lipman PW (1989) Geochemistry of intrusive rocks associated with the Latir volcanic field, New Mexico, and contrasts between evolution of plutonic and volcanic rocks. Contrib Mineral Petrol 103:90–109

Justet L, Spell TL (2001) Effusive eruptions from a large silicic magma chamber: the Bearhead Rhyolite, Jemez volcanic field, NM. J Volcanol Geotherm Res 107:241–264

Lanphere MA, Champion DE, Christiansen RL, Izett GA, Obradovich JD (2002) Revised ages for tuffs of the Yellowstone Plateau volcanic field: assignment of the Huckleberry Ridge Tuff to a new geomagnetic polarity event. Geol Soc Am Bull 114:559–568

LaTourette TZ, Burnett DS, Bacon CR (1991) Uranium and minor-element partitioning in Fe–Ti oxides and zircon from partially melted granodiorite, Crater Lake, Oregon. Geochim Cosmochim Acta 55:457–469

Leeman W, Phelps DW (1981) Partitioning of rare earths and other trace elements between sanidine and coexisting volcanic glass. J Geophys Res 86:10193–10199

Lowenstern JB, Persing HM, Wooden JL, Lanphere M Donnely-Nolan J, Grove TL (2000) U–Th dating of single zircons from young granitoid xenoliths: new tools for understanding volcanic processes. Earth Planet Sci Lett 183:291–302

Lowenstern JB, Charlier BLA, Wooden JL, Lanphere MA, Clynne MA, Bullen TD (2001) Isotopic constraints (U, Th, Pb, Sr, Ar) on the timing of magma generation, storage, and eruption of a late-Pleistocene subvolcanic granite, Alid volcanic center, Eritrea. EOS Trans Am Geophys Union 82: 1346

Ludwig KR, Tittertington DM (1994) Calculation of $^{230}Th/U$ isochrons, ages, and errors. Geochim Cosmochim Acta 58:5031–5042

Mahood GA (1990) Evidence for long residence times of rhyolitic magma in the Long Valley magmatic system: the isotopic record in the precaldera lavas of Glass Mountain: reply. Earth Planet Sci Lett 99:395–399

Mahood GA, Cornejo PC (1992) Evidence for ascent of differentiated liquids in a silicic magma chamber found in a granitic pluton. Trans R Soc Edinb 83:63–69

Miller CF, Mittlefehldt DW (1984) Extreme fractionation in felsic magma chambers: a product of liquid-state diffusion or fractional crystallization? Earth Planet Sci Lett 68:151–158

Newhall CG, Dzurisin D (1988) Historical unrest at large calderas of the world. US Geol Surv Bull 1855

Obradovich JD (1992) Geochronology of the late Cenozoic volcanism of Yellowstone National Park and adjoining areas, Wyoming and Idaho. US Geol Surv Open-File Rep 92-408

Reid MR, Coath CD (2000) In situ U–Pb ages of zircons from the Bishop Tuff: no evidence for long crystal residence times. Geology 28:443–446

Reid MR, Coath CD, Harrison TM, McKeegan KD (1997) Prolonged residence times for the youngest rhyolites associated with Long Valley Caldera: ^{230}Th–^{238}U ion microprobe dating of young zircon. Earth Planet Sci Lett 150:27–39

Robinson DM, Miller CF (1999) Record of magma chamber processes preserved in accessory mineral assemblages, Aztec Wash pluton, Nevada. Am Mineral 84:1346–1353

Shärer U (1984) The effect if initial ^{230}Th disequilibrium on young U–Pb ages: the Makalu case, Himalaya. Earth Planet Sci Lett 67:191–204

Sisson TW, Bacon CR (1999) Gas-driven filter pressing in magma. Geology 27:613–616

Smith RB (1979) Ash-flow magmatism. Geol Soc Am Spec Pap 180:5–27

Snyder D (2000) Thermal effects of the intrusion of basaltic magma into a more silicic magma chamber and implications for eruption triggering. Earth Planet Sci Lett 175:257–273

Sparks RSJ, Marshall LA (1986) Thermal and mechanical constraints on mixing between mafic and silicic magmas. J Volcanol Geotherm Res 29:99–124

Sparks RSJ, Huppert HE, Wilson CJN (1990) Evidence for long residence times of rhyolitic magma in the Long Valley magmatic system: the isotopic record in precaldera lavas of Glass Mountain: comment. Earth Planet Sci Lett 99:387–389

Spell TL, Thousand yearsle R, Thirwall MT, Campbell AR (1993) Isotopic and geochemical constraints on the evolution of postcaldera rhyolites in the Valles caldera, New Mexico. J Geophys Res 98:19723–19739

Sturchio NC, Binz CM, Lewis III CH (1987) Thorium–uranium disequilibrium in a geothermal discharge zone at Yellowstone. Geochim Cosmochim Acta 51:2025–2034

Sutton AN, Blake S, Wilson CJN, Charlier BLA (2000) Late Quaternary evolution of a hyperactive rhyolite magmatic system: Taupo volcanic centre, New Zealand. J Geol Soc Lond 157:537–552

Trial AF, Spera FJ (1990) Mechanisms for the generation of compositional heterogeneities in magma chambers. Geol Soc Am Bull 102:353

Watson EB (1996) Dissolution, growth and survival of zircons during crustal fusion: kinetic principles, geological models and implications for isotopic inheritance. Trans R Soc Edinb Earth Sci 87:43–56

Watson EB, Harrison TM (1983) Zircon saturation revisited: temperatures and composition effects in a variety of crustal magma types. Earth Planet Sci Lett 64:295–304

Wolff JA, Ramos FC, Davidson J (1999) Sr isotope disequilibrium during differentiation of the Bandelier Tuff: constraints on the crystallization of a large rhyolitic magma chamber. Geology 27:495–498